

G Protein-coupled Receptors and Resistance to Inhibitors of Cholinesterase-8A (Ric-8A) Both Regulate the Regulator of G Protein Signaling 14 (RGS14)·G α_{i1} Complex in Live Cells^{*[5]}

Received for publication, June 22, 2011, and in revised form, August 19, 2011. Published, JBC Papers in Press, August 31, 2011, DOI 10.1074/jbc.M111.274928

Christopher P. Vellano^{†1}, Ellen M. Maher[§], John R. Hepler[†], and Joe B. Blumer^{§2}

From the [†]Department of Pharmacology, Emory University School of Medicine, Atlanta, Georgia 30322 and the [§]Department of Cell and Molecular Pharmacology and Experimental Therapeutics, Medical University of South Carolina, Charleston, South Carolina 29425

Background: Regulator of G protein signaling 14 (RGS14) is a G protein regulatory (GPR) protein that participates in unconventional G protein signaling independent of G protein-coupled receptors (GPCRs).

Results: RGS14 forms regulated complexes with GPCRs in live cells.

Conclusion: RGS14 integrates unconventional and conventional GPCR-dependent G protein signaling pathways.

Significance: GPR proteins appear to be at the nexus of divergent G protein signaling pathways.

Regulator of G protein signaling 14 (RGS14) is a multifunctional scaffolding protein that integrates both conventional and unconventional G protein signaling pathways. Like other RGS (regulator of G protein signaling) proteins, RGS14 acts as a GTPase accelerating protein to terminate conventional G $\alpha_{i/o}$ signaling. However, unlike other RGS proteins, RGS14 also contains a G protein regulatory/GoLoco motif that specifically binds G $\alpha_{i1/3}$ -GDP in cells and *in vitro*. The non-receptor guanine nucleotide exchange factor Ric-8A can bind and act on the RGS14·G α_{i1} -GDP complex to play a role in unconventional G protein signaling independent of G protein-coupled receptors (GPCRs). Here we demonstrate that RGS14 forms a G $\alpha_{i/o}$ -dependent complex with a G $_i$ -linked GPCR and that this complex is regulated by receptor agonist and Ric-8A (resistance to inhibitors of cholinesterase-8A). Using live cell bioluminescence resonance energy transfer, we show that RGS14 functionally associates with the α_{2A} -adrenergic receptor (α_{2A} -AR) in a G $\alpha_{i/o}$ -dependent manner. This interaction is markedly disrupted after receptor stimulation by the specific agonist UK14304, suggesting complex dissociation or rearrangement. Agonist-mediated dissociation of the RGS14· α_{2A} -AR complex occurs in the presence of G $\alpha_{i/o}$ but not G α_s or G α_q . Unexpectedly, RGS14 does not dissociate from G α_{i1} in the presence of stimulated α_{2A} -AR, suggesting preservation of RGS14·G α_{i1} complexes after receptor activation. However, Ric-8A facilitates

dissociation of both the RGS14·G α_{i1} complex and the G α_{i1} -dependent RGS14· α_{2A} -AR complex after receptor activation. Together, these findings indicate that RGS14 can form complexes with GPCRs in cells that are dependent on G $\alpha_{i/o}$ and that these RGS14·G α_{i1} -GPCR complexes may be substrates for other signaling partners such as Ric-8A.

Established models of G protein signaling suggest that heterotrimeric G proteins (G $\alpha\beta\gamma$ subunits) are linked to specific G protein-coupled receptors (GPCRs),³ and that these receptors act as guanine nucleotide exchange factors (GEFs) toward the G α subunit to promote nucleotide exchange and downstream signaling events (1, 2). The regulators of G protein signaling (RGS) proteins act as GTPase accelerating proteins on the activated G α subunit, catalyzing GTP hydrolysis to terminate G protein signaling (3–5).

Recent studies have explored novel unconventional G protein signaling pathways involved with cell division and synaptic signaling/plasticity that can operate independently of GPCRs (6–13). The hallmark of these unconventional G protein pathways are signaling complexes involving G α -GDP bound to proteins containing one or more G protein regulatory (GPR) motifs. Resistance to inhibitors of cholinesterase 8A (Ric-8A) is a cytosolic GEF that directly promotes nucleotide exchange on G α_i , G α_o , and G α_q subunits in unconventional G protein signaling (14). Ric-8A also recognizes, binds, and regulates the formation/dissociation of some GPR·G α_{i1} -GDP complexes, such as AGS3·G α_{i1} -GDP, LGN·G α_{i1} -GDP, and RGS14·G α_{i1} -GDP (15–17).

RGS14 is a functionally and structurally complex signaling protein that is most highly expressed in the brain but also present in spleen, thymus, and lymphocytes (18–21). Within brain,

* This work was supported, in whole or in part, by National Institutes of Health Grants R01NS049195 and R01NS037112 (to J. R. H.), R01GM086510 (to C. P. V.), and Pharmacological Sciences Training Grant T32 GM008602 (to C. P. V.). This work was also supported by a PhRMA Foundation Pre-doctoral Pharmacology/Toxicology Fellowship (to C. P. V.). This research was also supported in part by the Microscopy Core of the Emory Neuroscience NINDS Core Facilities Grant P30NS055077.

[5] The on-line version of this article (available at <http://www.jbc.org>) contains supplemental Figs. S1 and S2.

¹ To whom correspondence may be addressed: Emory University School of Medicine, Dept. of Pharmacology, 1510 Clifton Rd., Rollins Research Center G205, Atlanta, GA 30322. Tel.: 404-727-8192; E-mail: cvellan@emory.edu.

² To whom correspondence may be addressed: Medical University of South Carolina, Dept. of Cell and Molecular Pharmacology and Experimental Therapeutics, 114 Doughty St., STB331, Charleston, SC 29425. Tel.: 843-792-7138; E-mail: blumerjb@musc.edu.

³ The abbreviations used are: GPCR, G protein-coupled receptors; GEF, guanine nucleotide exchange factor; RGS, regulators of G protein signaling; GPR, G protein regulatory; Ric-8A, resistance to inhibitors of cholinesterase 8A; AGS, activators of G protein signaling; BRET, bioluminescence resonance energy transfer; AR, adrenergic receptor; PTX, pertussis toxin.

Ric-8A and GPCR Regulation of the RGS14-G α_{i1} Complex

RGS14 is predominately localized in the CA2 subregion of the hippocampus, where it is involved in spatial memory, learning, and synaptic plasticity (22). The unique structure of RGS14, which includes an RGS domain, two Ras/Rap binding domains, and a GPR (also known as GoLoco (23)) motif (20, 21) suggests that RGS14 functions in the brain through a variety of signaling mechanisms that may involve both G protein and MAP kinase signaling cascades (24). In addition to possessing GTPase accelerating protein activity toward activated G $\alpha_{i/o}$ -GTP subunits, RGS14 also exhibits selective guanine nucleotide dissociation inhibitor activity toward G $\alpha_{i1/3}$ -GDP subunits through direct binding of its GPR motif (18, 19, 21, 25–27). In this regard RGS14 shares similarities with the family of Group II activators of G protein signaling (AGS) proteins that are characterized by one or more GPR motifs and mediate unconventional G protein signaling (28–30). Similar to AGS3 and LGN, which form stable complexes with G α_{i1} -GDP via their GPR motifs (15, 16), the RGS14-G α_{i1} -GDP signaling complex is a substrate for Ric-8A-induced dissociation and nucleotide exchange on the resulting free G α_{i1} (17).

Recent evidence suggests that unconventional pathways involving GPR-G α -GDP complexes and conventional pathways involving GPCR-G protein complexes may be functionally linked. In particular, the GPR proteins AGS3 and AGS4 appear to interface with GPCRs in a G α_i -dependent manner (31, 32). Compelling evidence also indicates that RGS proteins directly and selectively interact with GPCRs to modulate G protein signaling (for review, see Ref. 33). Given that RGS14 is an RGS protein that interacts with G $\alpha_{i/o}$ -GTP but contains a GPR motif that binds G $\alpha_{i1/3}$ -GDP, we examined whether the RGS14-G α_{i1} complex can be regulated by a G $\alpha_{i/o}$ -linked GPCR.

The non-receptor GEF Ric-8A regulates the RGS14-G α_{i1} complex (17) as well as certain GPCR signaling pathways (34, 35). However, it remains unknown whether Ric-8A can modulate GPCR-G α interactions, especially in the presence of a GPR protein such as RGS14. Therefore, we also studied the effects of Ric-8A on RGS14-G α_{i1} -GPCR complex formation and whether RGS14 may be at the interface between conventional and unconventional G protein signaling pathways. Here we report the first evidence that the RGS14-G α_{i1} -GDP complex is regulated in concert by both a G $\alpha_{i/o}$ -linked GPCR and Ric-8A in live cells. We show that RGS14 forms a stable complex with G α_{i1} via its GPR motif and that this complex is proximal to GPCRs as evidenced by the presence of specific bioluminescence resonance energy transfer (BRET) signals between RGS14 and the α_{2A} -adrenergic receptor (α_{2A} -AR) in the presence of G α_{i1} . This RGS14- α_{2A} -AR complex partially dissociates/rearranges after receptor agonist treatment and is further regulated by Ric-8A. Together, these findings illustrate that RGS14 functions together in both conventional and unconventional G protein signaling and that Ric-8A may recognize and act on GPCR-G α_i -GPCR complexes to further regulate G α_i signaling.

EXPERIMENTAL PROCEDURES

Plasmids and Antibodies—The rat RGS14 cDNA used in this study (GenBankTM accession number U92279) was acquired as described (19). Rat RGS14 was used as a template in PCR reactions using *TaKaRa Taq* (Fisher) to generate *Renilla* luciferase

(Luc) fusion protein constructs in the pRLucN2 vector graciously provided by Dr. Michel Bouvier (University of Montreal). The following oligonucleotides and restriction enzymes were used in the PCR amplification and subsequent digestion: RGS14 forward primer 5'-GCT CTC GAG GCC ACC ATG CCA GGG AAG CCC AAG CAC-3', XhoI; reverse primer 5'-CGC GGT ACC TGG TGG AGC CTC CTG AGA ACC-3', KpnI.

The RGS14-Luc GPR mutant, in which invariant glutamine and arginine residues (Gln⁵¹⁵ and Arg⁵¹⁶) were both mutated to alanine, was generated by site-directed mutagenesis using a Stratagene site-directed mutagenesis kit according to the manufacturer's instructions and is referred to as RGS14(*GPR-null*). Oligonucleotide primers used to create RGS14-Q515A/R516A-Luc (RGS14(*GPR-null*)) are as follows: RGS14(*GPR-null*) forward primer 5'-GGG GCC CAT GAC GCC GCC GGA CTT CTT CGC AAA G-3' and reverse primer 5'-CTT TGC GAA GTC CGG CGG CGT CAT GGG CCC C-3'. The RGS14-Luc RGS domain mutant, in which invariant glutamic acid and asparagine (Glu⁹² and Asn⁹³) residues were both mutated to alanine, was generated by site-directed mutagenesis using a Stratagene kit and is referred to as RGS14(*RGS-null*). Oligonucleotide primers used to create RGS14-E92A/N93A-Luc (RGS14(*RGS-null*)) are as follows: RGS14(*RGS-null*) forward primer 5'-AAG GAA TTC AGC GCC GCC GCC GTA ACT TTC TGG CAA GC-3' and reverse primer 5'-GCT TGC CAG AAA GTT ACG GCG GCG GCG CTG AAT TCC TT-3'. The RGS14-Luc RGS/GPR double mutant referred to as RGS14(*RGS/GPR-null*) was generated by using RGS14(*RGS-null*) as a template and RGS14(*GPR-null*) primers in site-directed mutagenesis. In all cases, the plasmids were sequenced to confirm the fidelity of the PCR.

Wild-type AGS4-Luc was generated as previously described (32). Rat G α_{i1} -YFP (G α_{i1} -YFP) in pcDNA3.1 was generated by Dr. Gibson (36) and was generously provided along with pcDNA3.1::Ric-8A plasmid by Dr. Gregory Tall (University of Rochester School of Medicine and Dentistry). G α_{i1} -N149I-YFP (referred to as G α_{i1} -GPRi), G α_{i1} -G183S-YFP (referred to as G α_{i1} -RGSi), and G α_{i1} -G183S/N149I-YFP (referred to as G α_{i1} -RGSi/GPRi) were generated using the QuikChange kit (Stratagene) previously described. pcDNA3.1::G α_{i1} -YFP was used as a template for oligonucleotide primers G α_{i1} -GPRi forward primer 5'-GGG AGT ACC AGC TGC TCG ATT CGG CGG CGT A-3' and reverse primer 5'-TAC GCC GCC GAA TCG ATC AGC TGG TAC TCC C-3' and G α_{i1} -RGSi forward primer 5'-AGT GAA AAC GAC GTC AAT TGT GGA AA-3' and reverse primer 5'-GGT TTC CAC AAT TGA CGT CGT TTT CA-3'. The G α_{i1} -RGSi/GPRi double mutant was constructed using the G α_{i1} -GPRi as a template for the G α_{i1} -RGSi primers. In all cases, the plasmids were sequenced to confirm the fidelity of the PCR.

G α_s -YFP and G α_q -YFP constructs were obtained from Dr. Catherine Berlot (Geisenger Institute, Danville, PA). Glu-Glu-tagged recombinant G α_{i1} plasmid was purchased from UMR cDNA Resource Center (Rolla, Missouri). α_{2A} -AR and β_2 -AR plasmids were generated as described and provided by Dr. Michel Bouvier (University of Montreal) (37, 38).

Anti-sera used include anti-G α_{i1} (Millipore and Santa Cruz Biotechnologies, Inc.), anti-G α_{i2} (Abcam), anti-G α_{i3} and anti-G α_s (gifts from Dr. Thomas Gettys at Pennington Biomedical Research Center, Baton Rouge, LA), anti-FLAG (Sigma), anti-Ric-8A (provided by Dr. Gregory Tall, University of Rochester School of Medicine and Dentistry), anti-G α_q (Santa Cruz Biotechnologies, Inc.), anti-G α_o (Santa Cruz Biotechnologies, Inc.), Alexa 546 goat anti-rabbit secondary IgG (Invitrogen), Alexa 633 goat anti-mouse secondary IgG (Invitrogen), peroxidase-conjugated goat anti-mouse IgG (Rockland Immunochemicals, Inc.), and peroxidase-conjugated goat anti-rabbit IgG (Bio-Rad).

Cell Culture and Transfection—HEK293 cells were maintained in Dulbecco's minimal essential medium (without phenol red) containing 10% fetal bovine serum (5% after transfection), 2 mM glutamine, 100 units/ml penicillin, and 100 mg/ml streptomycin. Cells were incubated at 37 °C with 5% CO₂ in a humidified environment. Transfections were performed using previously described protocols with polyethyleneimine (Polysciences, Inc.) (32). For immunofluorescence, cells were seeded onto glass coverslips before transfection.

BRET—BRET experiments were performed as previously described (31, 32). Briefly, HEK293 cells were transiently transfected with BRET donor and acceptor plasmids using polyethyleneimine. Forty-eight hours after transfection, the culture medium was removed, and cells were washed once with PBS and harvested with Tyrode's solution (140 mM NaCl, 5 mM KCl, 1 mM MgCl₂, 1 mM CaCl₂, 0.37 mM NaH₂PO₄, 24 mM NaHCO₃, 10 mM HEPES, and 0.1% glucose (w/v), pH 7.4). Each group of cells was distributed into gray 96-well OptiPlates (PerkinElmer Life Sciences) in triplicate, with each well containing 1 × 10⁵ cells. The acceptor (YFP/Venus-tagged) protein expression levels were evaluated by measuring total fluorescence using the TriStar LB 941 plate reader (Berthold Technologies) with excitation and emission filters at 485 and 535 nm, respectively. Data were analyzed using the MikroWin 2000 program. After fluorescence measurement, coelenterazine H (Nanolight Technology; 5 μM final concentration) was added and luminescence detected in the 480 ± 20 and 530 ± 20 nm windows for donor (Luc) and acceptor (YFP/Venus), respectively, by the TriStar LB 941 plate reader. BRET signals were determined by calculating the ratio of the light intensity emitted by the YFP/Venus divided by the light intensity emitted by Luc. Net BRET values were corrected by subtracting the background BRET signal detected from the expression of the donor fusion protein (Luc) alone. Agonists used were UK14304 (Sigma) and isoproterenol (Sigma). Immunoblots were performed as described previously (39).

Immunofluorescence and Confocal Imaging—Transfected HEK293 cells were treated with either vehicle or 10 μM UK14304 diluted in serum-free DMEM for 5 min at 37 °C. Cells were then fixed at room temperature for 15 min in buffer containing 3.7% paraformaldehyde diluted in PBS. Cells were washed in PBS and incubated for 8 min with 0.4% Triton X-100 diluted in PBS. Cells were then blocked for 1 h at room temperature in PBS containing 10% goat serum and 3% bovine serum albumin. Next, cells were incubated in this same buffer with a 1:1000 dilution of rabbit anti-FLAG and/or mouse anti-G α_{i1}

antibodies at room temperature for 2 h. Cells were washed with PBS (3×) and incubated with 1:300 dilutions of Alexa 546 goat anti-rabbit and/or Alexa 633 goat anti-mouse secondary antibodies at room temperature for 1 h. Cells were washed with PBS again (3×) and mounted with ProLong Gold Antifade Reagent (Invitrogen). Confocal images were taken using a 63× oil immersion objective from a LSM510 laser scanning microscope with AxioObserver Stand (Zeiss). Images were processed using the ZEN 2009 Light Edition software and Adobe Photoshop 7.0 (Adobe Systems).

RESULTS

RGS14 Interacts Selectively with G α_{i1} through Its GPR Motif—RGS14 has two distinct G α -binding domains. The RGS domain binds activated G $\alpha_{i/o}$ subunits (18, 19, 21), whereas the GPR motif binds inactive G α_{i1} and G α_{i3} (19, 26, 27, 40). That RGS14 is recruited from the cytosol to the plasma membrane and colocalizes with wild-type G α_{i1} (Fig. 1A, supplemental Fig. S1, and Refs. 17 and 27) suggests that RGS14 forms a stable complex with G α_{i1} at the plasma membrane, which we sought to quantitatively measure using BRET. We therefore measured the strength and selectivity of a BRET signal between RGS14-Luc and various YFP-tagged G α subunits (36, 41–43) (Fig. 1B). Of note, the YFP tag was inserted into the loop joining the α B and α C helices of each G α (36, 41, 43), preserving nucleotide binding and hydrolysis properties similar to the wild-type protein (36). Transfection of HEK cells with increasing amounts of G α -YFP plasmid and a fixed amount (5 ng) of RGS14-Luc plasmid showed a robust, saturable BRET signal in the presence of G α_{i1} -YFP, whereas no BRET signal was observed between RGS14-Luc paired with either G α_s -YFP or G α_q -YFP (Fig. 1B). This BRET signal saturation is indicative of a specific interaction between RGS14 and G α_{i1} (44).

To further show BRET signal selectivity for RGS14-Luc interactions with G α_{i1} -YFP, we performed a competition assay in cells co-expressing untagged G α subunits (Fig. 1C) to determine which G α subunits could displace G α_{i1} -YFP from RGS14-Luc and disrupt the BRET signal. As expected, the previously reported RGS14 binding partners G α_{i1} and G α_{i3} each disrupted the RGS14/G α_{i1} BRET signal, indicative of competition with G α_{i1} -YFP for RGS14 binding. By contrast, G α_{i2} , G α_o , G α_s , and G α_q did not disrupt G α_{i1} -YFP binding to RGS14. This selectivity for G α_{i1} and G α_{i3} binding is entirely consistent with earlier reports showing RGS14 binding to only G α_{i1} and G α_{i3} but not other G α through its GPR motif, further validating our BRET system (18, 19, 21, 26, 27, 40).

Findings in Fig. 1 suggested that the BRET signal we observed between RGS14 and G α_{i1} occurs via the GPR motif. To test this hypothesis, we constructed mutants of RGS14-Luc that rendered it insensitive to binding G α_{i1} -YFP through either the RGS domain (RGS14-E92A/N93A-Luc; *RGS-null*) (18), the GPR motif (RGS14-Q515A/R516A-Luc; *GPR-null*) (25, 45), or both (RGS14-E92A/N93A/Q515A/R516A-Luc; *RGS/GPR-null*) (Fig. 2, A and B). The BRET signal between wild-type RGS14 (WT) and G α_{i1} was comparable with that between RGS14(*RGS-null*) and G α_{i1} , suggesting that the majority of the observed BRET signal was not due to the RGS domain interacting with G α_{i1} . However, the BRET signal between RGS14(*GPR-*

Ric-8A and GPCR Regulation of the RGS14-G α_{i1} Complex

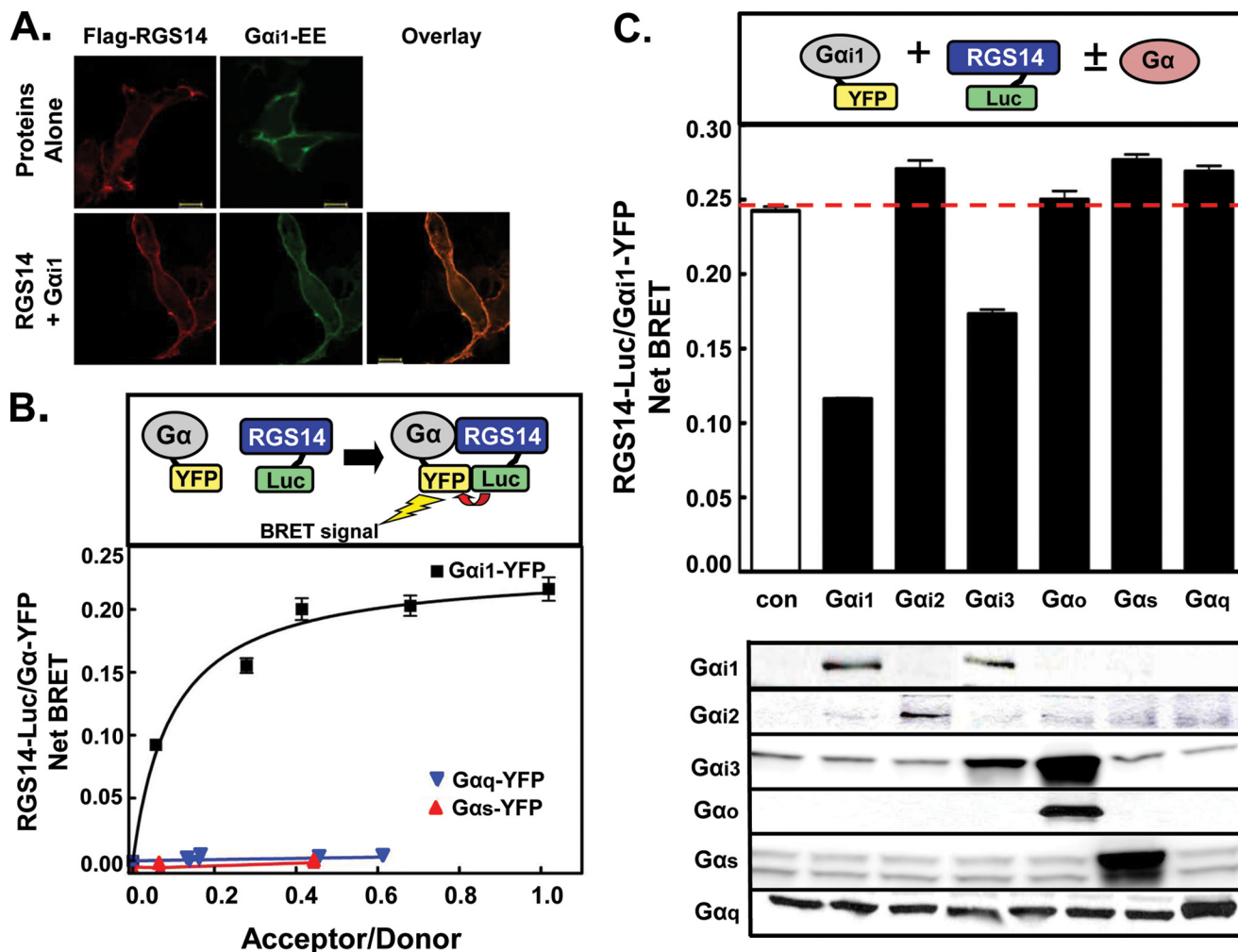


FIGURE 1. RGS14 selectively interacts with G α_{i1} and G α_{i3} in the basal state of live cells as observed by BRET. *A*, FLAG-RGS14 and G α_{i1} -Glu-Glu (G α_{i1} -EE) plasmids were transfected into HEK cells alone and in combination. Cells were fixed, subjected to immunocytochemistry, and analyzed using confocal microscopy with a 63 \times objective as described under "Experimental Procedures." Images are representative of cells observed in three separate experiments. Scale bars represent 10 μ m. *B*, top, a diagram shows the principle of BRET using the RGS14-Luc/G α_{i1} -YFP pair. Non-radiative emission from the Luc tag excites the YFP if the donor/acceptor pairs are <100 Å, which then emits at 535 nm. Bottom, HEK cells were transfected with 5 ng RGS14-Luc plasmid alone or in combination with 10, 50, 100, 250, or 500 ng of either G α_{i1} -YFP, G α_s -YFP, or G α_q -YFP plasmid. BRET signals (luminescence measured: donor, 480 \pm 20 nm; acceptor, 530 \pm 20 nm) were measured, and net BRET was calculated by first calculating the 530 \pm 20/480 \pm 20 nm ratio and then subtracting the background BRET signal determined from cells transfected with the RGS14-Luc plasmid alone. *C*, top panel, HEK cells were transfected with 5 ng of RGS14-Luc and 250 ng of G α_{i1} -YFP plasmids alone (con) or in combination with 1 μ g of untagged G α_{i1} , G α_{i2} , G α_{i3} , G α_o , G α_s , or G α_q plasmid. Net BRET signals are shown between RGS14-Luc and G α_{i1} -YFP. Bottom panel, shown is a representative immunoblot of the different untagged G α subunits used in the BRET experiment. All BRET graphs are representative of at least three separate experiments.

null) and G α_{i1} was \sim 5-fold lower than that of the RGS14-WT/G α_{i1} pair. This indicates that the observed BRET signal between RGS14 and G α_{i1} is primarily due to the GPR motif. As an additional approach, we generated G α_{i1} -YFP mutants that were insensitive to binding either the RGS domain (G α_{i1} -G183S-YFP; RGSi) (46), the GPR motif (G α_{i1} -N149I-YFP; GPRi) (47, 48), or both (G α_{i1} -G183S/N149I-YFP; RGSi/GPRi) (Fig. 2C). Consistent with findings in Fig. 2B, the BRET signal between RGS14 and G α_{i1} -GPRi was substantially (\sim 8-fold) lower than that generated by RGS14 paired with either wild-type G α_{i1} (WT) or G α_{i1} -RGSi. Taken together, these findings are entirely consistent with the idea that the majority of the BRET signals observed between RGS14 and G α_{i1} are due to the interaction between the RGS14 GPR motif and G α_{i1} .

RGS14 Forms a Complex with the α_{2A} -Adrenergic Receptor in a G α_{i1} -Dependent Manner—The GPR proteins AGS3 and AGS4 form G α_i -dependent complexes with GPCRs that are

regulated by receptor activation (31, 32). Therefore, we sought to investigate whether the RGS14-G α_{i1} complex can also be regulated by GPCRs in cells. Subcellular localization data showed that although RGS14 remained predominately cytosolic in the presence of co-expressed α_{2A} -AR, it was recruited to the plasma membrane in the presence of both overexpressed α_{2A} -AR and G α_{i1} in the absence of agonist (Fig. 3, left panel). This suggests formation of an RGS14-G α_{i1} - α_{2A} -AR complex at the plasma membrane. Although RGS14 and G α_{i1} remained at the plasma membrane, the α_{2A} -AR internalized in the presence of agonist UK14304 (Fig. 3, right panel).

To further examine the regulatory effects of GPCRs on RGS14-G α_{i1} complexes, we analyzed the BRET signals between RGS14-Luc and Venus-tagged α_{2A} -AR or β_2 -AR (Fig. 4). As expected, little to no detectable BRET signal was observed between RGS14 and the G $_s$ -linked β_2 -AR in the absence or presence of both G α_{i1} and the receptor agonist isoproterenol

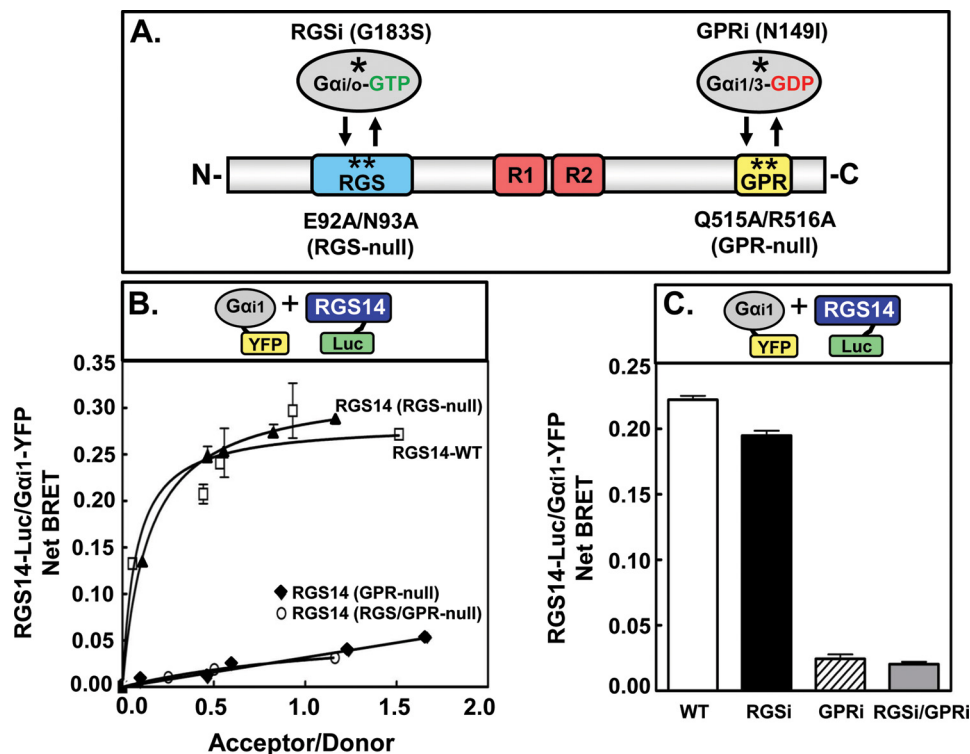


FIGURE 2. **RGS14 BRET signals with Gα_{i1} in live cells are dependent on the GPR motif.** A, shown is an illustration of the functional RGS14 and Gα_{i1} mutants, with Gα_{i/o}-RGSi incapable of binding the RGS domain, Gα_{i1/3}-GPRi incapable of binding the GPR motif, RGS14(RGS-null) incapable of binding active Gα_{i/o} and RGS14(GPR-null) incapable of binding inactive Gα_{i1/3}. B, HEK cells were transfected with increasing amounts of Gα_{i1}-YFP plasmid (10, 50, 100, 250, and 500 ng) in combination with 5 ng of either wild-type RGS14-Luc (RGS14-WT), RGS14(RGS-null)-Luc, RGS14(GPR-null)-Luc, or RGS14(RGS/GPR-null)-Luc plasmids. Net BRET was calculated by first calculating the 530 ± 20/480 ± 20-nm ratio and then subtracting the background BRET signal determined from cells transfected with the RGS14-Luc expression vector alone. Net BRET is shown between Gα_{i1}-YFP and the different RGS14-Luc mutants. This figure is representative of at least three separate experiments with triplicate determinations. C, HEK cells were transfected with 5 ng of wild-type RGS14-Luc and 250 ng of either wild-type Gα_{i1}-YFP (WT), Gα_{i1}-RGSi-YFP, Gα_{i1}-GPRi-YFP, or Gα_{i1}-RGSi/GPRi-YFP plasmids. Net BRET is shown between RGS14-Luc and the different Gα_{i1}-YFP mutants. These data are expressed as the mean of six separate experiments with triplicate determinations. *, point mutations in the proteins.

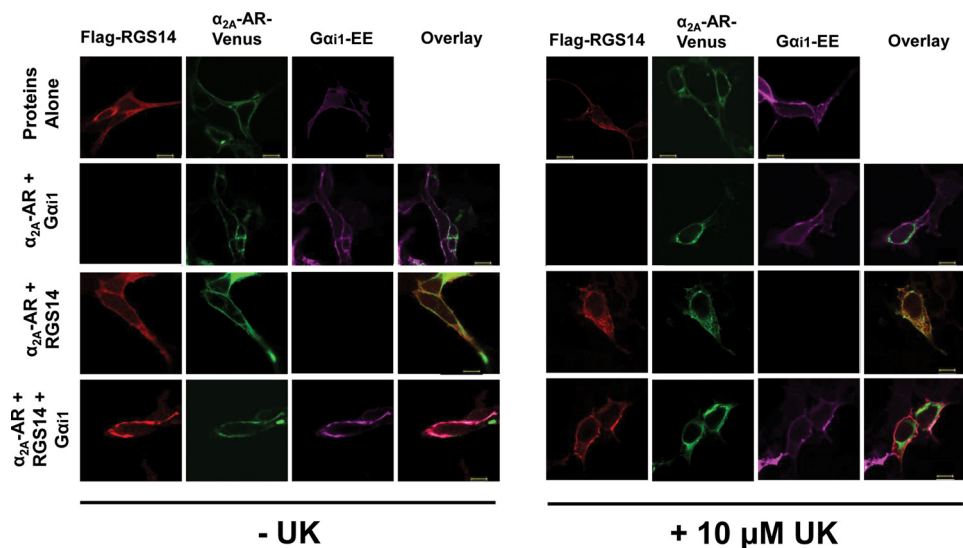


FIGURE 3. **RGS14 co-localization with Gα_{i1} and the α_{2A}-AR in live cells is regulated by receptor agonist.** FLAG-RGS14, Gα_{i1}-Glu-Glu (Gα_{i1}-EE), and α_{2A}-AR-Venus were transfected into HEK cells alone and in combination. Cells were either unstimulated (-UK) or stimulated (+UK) with 10 μM UK14304 for 5 min. Cells were fixed, subjected to immunocytochemistry, and analyzed using confocal microscopy as described under "Experimental Procedures." Images are representative of cells observed in three separate experiments. Scale bars represent 10 μm.

(Fig. 4A). Very low specific BRET signals were observed between RGS14 and α_{2A}-AR both in the absence and presence of receptor agonist UK14304 (Fig. 4B, filled circles and open circles, respectively). However, a 3-fold increase in BRET signal was observed between α_{2A}-AR and RGS14 in the presence of

co-expressed Gα_{i1} (Fig. 4B, filled triangles). This signal was reduced by ~50% in the presence of UK14304 (Fig. 4B, open triangles). This agonist-induced reduction in BRET correlates with the lack of co-localization between RGS14 and the α_{2A}-AR after agonist stimulation (Fig. 3, right panel). Furthermore, ago-

Ric-8A and GPCR Regulation of the RGS14-G α_{i1} Complex

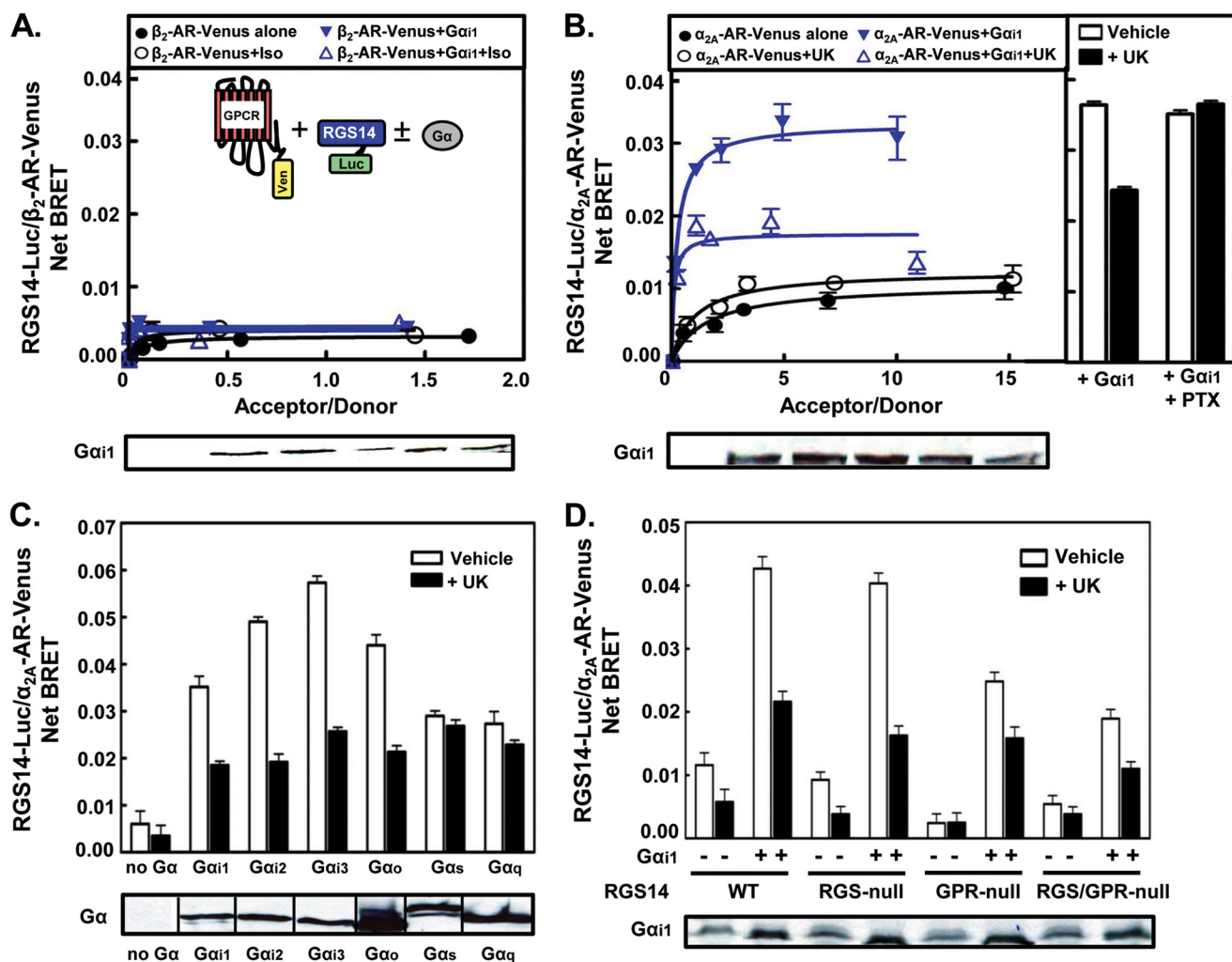


FIGURE 4. RGS14 forms a $G\alpha_{i1o}$ -dependent complex with the α_{2A} -AR in live cells. *A*, Net BRET signals are shown from HEK cells transfected with 5 ng of RGS14-Luc and 0, 10, 50, 100, 250, or 500 ng of β_2 -AR-Venus plasmids in the presence or absence of 750 ng pcDNA3:: $G\alpha_{i1}$. Measurements were taken after treatment with either vehicle or isoproterenol (100 μ M) for 5 min. A schematic representing the BRET principle used in all experiments of Fig. 4, which includes BRET measured between RGS14-Luc and a GPCR-Venus (Ven) in the presence or absence of untagged $G\alpha$, is shown within the graph. *B*, *left panel*, Net BRET signals are shown from HEK cells transfected with 5 ng of RGS14-Luc and either 0, 10, 50, 100, 250, or 500 ng of α_{2A} -AR-Venus plasmid in the presence or absence of 750 ng of pcDNA3:: $G\alpha_{i1}$. Measurements were taken after treatment with either vehicle or α_{2A} -AR agonist UK14304 (10 μ M) for 5 min. *Bottom panel*, shown are representative immunoblots of untagged $G\alpha_{i1}$ subunits used in samples with transfected $G\alpha_{i1}$. *Right panel*, Net RGS14-Luc/ α_{2A} -AR-Venus BRET signals are shown from HEK cells transfected with 5 ng of RGS14-Luc, 250 ng of α_{2A} -AR-Venus, and 750 ng of $G\alpha_{i1}$ plasmids. Measurements were taken after treatment with UK14304 for 5 min in the absence or presence of 100 ng/ml pertussis toxin that was applied 18 h before agonist treatment, as indicated in the figure. Data are expressed as the mean of three separate experiments with triplicate determinations. *C*, *top panel*, HEK cells were transfected with 5 ng of RGS14-Luc and 100 ng of α_{2A} -AR-Venus plasmids alone (no $G\alpha$) or in combination with 750 ng of either untagged $G\alpha_{i1}$, $G\alpha_{i2}$, $G\alpha_{i3}$, $G\alpha_o$, $G\alpha_s$, or $G\alpha_q$ plasmids. Cells were either treated with vehicle or UK14304 (10 μ M) for 5 min. The net BRET between RGS14-Luc and the α_{2A} -AR-Venus under each condition is shown. Data are expressed as the mean of three separate experiments with triplicate determinations. *Bottom panel*, shown is a representative immunoblot of the different $G\alpha$ subunits used. *D*, Net BRET signals for the RGS14-Luc/ α_{2A} -AR-Venus pair are shown for HEK cells transfected with 100 ng of α_{2A} -AR-Venus and combinations of 5 ng RGS14-Luc mutant (WT, RGS-null, GPR-null, and RGS/GPR-null) plasmids in the absence or presence of 750 ng of untagged pcDNA3:: $G\alpha_{i1}$, and then treated with either vehicle or 10 μ M UK14304 for 5 min. *Bottom panel*, shown is a representative immunoblot for $G\alpha_{i1}$ expression. Data are expressed as the mean of four separate experiments with triplicate determinations. The net BRET between RGS14-Luc and the GPCR-Venus pairs was calculated by first calculating the $530 \pm 20/480 \pm 20$ -nm ratio and then subtracting the background BRET signal determined from cells transfected with RGS14-Luc plasmid alone.

nist-induced dissociation of the RGS14- α_{2A} -AR complex was completely blocked by pretreatment with pertussis toxin (PTX) (Fig. 4*B*, *right panel*). The very low BRET signals observed between RGS14 and the β_2 -AR in the presence of $G\alpha_{i1}$ (Fig. 4*A*) illustrate that the BRET signals observed between RGS14 and the α_{2A} -AR are indeed specific and are not simply the result of “bystander BRET,” *i.e.* RGS14 localizing at the plasma membrane with $G\alpha_{i1}$ and randomly interacting with the receptor.

The interaction between RGS14 and the α_{2A} -AR was dependent on the presence of $G\alpha_{i/o}$ family members (Fig. 4*C*). Specific BRET signals were observed between RGS14 and the

α_{2A} -AR in the presence of $G\alpha_{i1}$, $G\alpha_{i2}$, $G\alpha_{i3}$, and $G\alpha_o$, with lower signals observed in the presence of $G\alpha_s$ and $G\alpha_q$. The agonist-mediated dissociation of the RGS14- α_{2A} -AR complex was observed in the presence of all four $G\alpha_{i/o}$ family members tested but not $G\alpha_s$ or $G\alpha_q$ (Fig. 4*C*).

To determine which domains of RGS14 are important for associating with the α_{2A} -AR, we performed BRET experiments using the RGS14 constructs with mutations in the RGS domain and GPR motif as described in Fig. 2*B* (Fig. 4*D*). BRET signals observed between either RGS14-WT or RGS14(RGS-null) and the α_{2A} -AR in the presence of co-expressed $G\alpha_{i1}$ were compa-

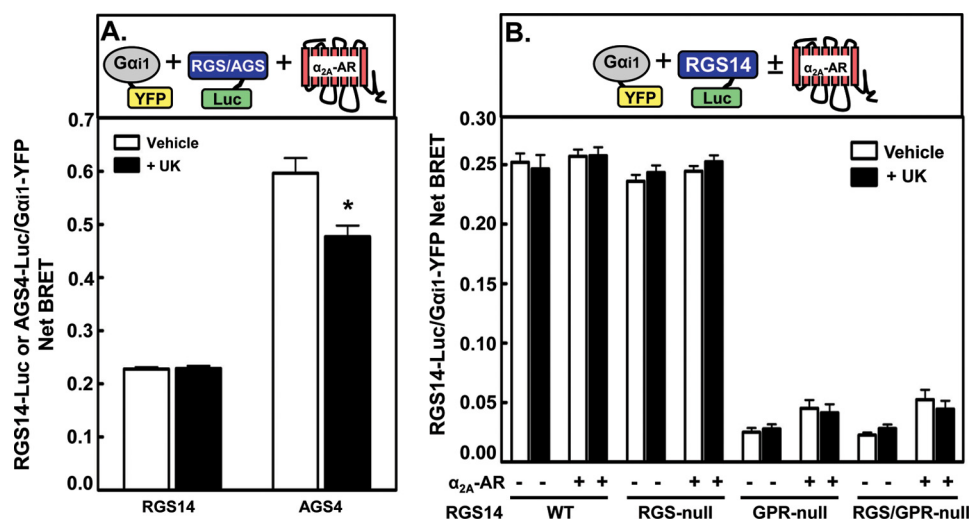


FIGURE 5. RGS14 remains bound to Gα₁₁ after α_{2A}-AR activation in live cells. *A*, HEK cells were transfected with 500 ng of untagged α_{2A}-AR, 250 ng Gα₁₁-YFP, and either 5 ng of RGS14-Luc or 2 ng of AGS4-Luc plasmids. Cells were treated with either vehicle or UK14304 (10 μM) for 5 min. Net BRET generated from the RGS14-Luc/Gα₁₁-YFP or AGS4-Luc/Gα₁₁-YFP pairs was calculated by first calculating the 530 ± 20/480 ± 20-nm ratio and then subtracting the background BRET signal determined from cells transfected with RGS14-Luc or AGS4-Luc plasmid alone, respectively. Data were analyzed using paired Student's *t* test. *, *p* < 0.05 as compared with vehicle control. *B*, HEK cells were transfected with 250 ng of Gα₁₁-YFP and 5 ng of RGS14-Luc (WT, RGS-null, GPR-null, and RGS/GPR-null) plasmids with and without 500 ng of untagged α_{2A}-AR plasmid and then treated with either vehicle or UK14304 (10 μM) for 5 min. Net BRET generated from the RGS14-Luc/Gα₁₁-YFP pair was calculated as in *A*. All data are expressed as the mean of three separate experiments with triplicate determinations.

rable, with similar reductions in response to receptor agonist UK14304. This suggests that the RGS domain of RGS14 is not required for the formation of the Gα₁₁-dependent complex with the α_{2A}-AR. In contrast, the BRET signals observed between the α_{2A}-AR and RGS14(*GPR-null*) in the presence of Gα₁₁ were reduced by ~50% in the absence of agonist compared with RGS14-WT, indicating that the GPR motif is critical to forming a complex with the α_{2A}-AR in the presence of Gα₁₁. Together, these results indicate that RGS14 forms a complex with the α_{2A}-AR in the presence of a Gα₁₁ protein and that the GPR motif is critical in promoting the formation of this complex (see supplemental Fig. S2A).

The RGS14·Gα₁₁ Complex Remains Intact after α_{2A}-AR Stimulation—Because the presence of Gα₁₁ promotes the formation of an RGS14·α_{2A}-AR complex that is regulated by agonist, we examined the effects of α_{2A}-AR stimulation on the RGS14·Gα₁₁ complex (Fig. 5). To test this, we measured the BRET signal between RGS14-Luc and Gα₁₁-YFP in the presence of untagged α_{2A}-AR. The RGS14·Gα₁₁ complex remains intact in the presence of the α_{2A}-AR regardless of receptor stimulation (Fig. 5A). This is in marked contrast to the decrease in BRET signal observed between AGS4-Luc and Gα₁₁-YFP in the presence of stimulated α_{2A}-AR (Fig. 5A and Ref. 32). Together, these findings suggest that the α_{2A}-AR dissociates from RGS14 after agonist stimulation but that the dissociated RGS14 remains in complex with Gα₁₁ (supplemental Fig. S2B). This portrays a novel mechanism of GPCR·Gα₁₁ complex function with GPCRs that may be unique to RGS14 compared with other Group II AGS proteins.

The GPR motif is still critical for RGS14 interactions with Gα₁₁ in the presence of the α_{2A}-AR (Fig. 5B), as >80% reductions in BRET signals were observed between Gα₁₁ and both RGS14(*GPR-null*) and RGS14(*RGS/GPR-null*) regardless of the presence of receptor. This indicates that even the presence of a

GPCR cannot facilitate RGS14 interactions with Gα₁₁ in the absence of a functional GPR motif.

Ric-8A Promotes Dissociation of the RGS14·Gα₁₁ Complex—Because we observed Ric-8A regulation of RGS14·Gα₁₁ complexes *in vitro* (17), we sought to quantitatively measure Ric-8A-mediated dissociation of RGS14·Gα₁₁ complexes in live cells using BRET (Fig. 6A). As expected (17), increasing Ric-8A protein levels induced a decrease in BRET between RGS14-Luc and Gα₁₁-YFP (Fig. 6C). Ric-8A-induced reductions in RGS14/Gα₁₁ BRET were inhibited by pertussis toxin (+PTX) (Fig. 6C), which blocks Ric-8A binding and GEF activity toward Gα₁₁ subunits (49). Expression of Ric-8A also induces an increase in Gα₁₁-YFP protein expression levels (Fig. 6B), which is consistent with recent evidence showing that Ric-8A is important for the functional expression and stability of Gα subunits (50). Interestingly, the effect of Ric-8A on Gα₁₁-YFP expression levels was not blocked by pertussis toxin pretreatment, suggesting that the effect of Ric-8A on Gα₁₁ expression is independent from its GEF activity.

We next studied the effects of Ric-8A on RGS14·Gα₁₁ complexes in the presence of the α_{2A}-AR (Fig. 7A). In the absence of Ric-8A, RGS14·Gα₁₁ complexes remained intact after receptor stimulation as before (see Fig. 5A). In the absence of receptor agonist, Ric-8A promoted a decrease in the RGS14/Gα₁₁ BRET signal. In the presence of agonist, Ric-8A induced an even greater decrease in the BRET signal (Fig. 7A). These findings suggest that Ric-8A can recognize and act on RGS14·Gα₁₁ complexes in the presence of GPCRs and even more so in the presence of activated receptors.

Ric-8A Potentiates Dissociation of the RGS14·α_{2A}-AR Complex Caused by Receptor Agonist—Because Ric-8A induced dissociation of Gα₁₁ from RGS14 in the presence of the α_{2A}-AR, we next investigated the effect of Ric-8A on the RGS14·α_{2A}-AR complex in the presence of Gα₁₁ (Fig. 7B). Ric-8A had little

Ric-8A and GPCR Regulation of the RGS14·Gα_{i1} Complex

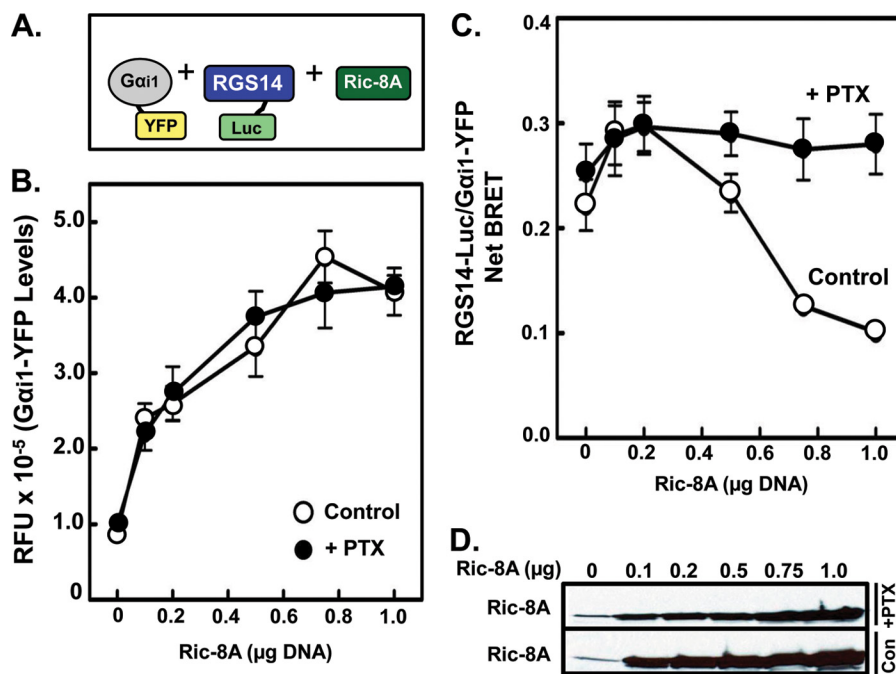


FIGURE 6. Ric-8A facilitates dissociation of RGS14 from Gα_{i1} in live cells. *A*, shown is a diagram illustrating the BRET measured in this experiment between RGS14-Luc and Gα_{i1}-YFP in the presence of untagged Ric-8A. *B*, HEK cells were transfected with 5 ng of RGS14-Luc, 250 ng of Gα_{i1}-YFP, and increasing amounts (0, 100, 200, 500, 750, or 1000 ng) of Ric-8A plasmids. Cells were subsequently left untreated or pretreated with 100 ng/ml pertussis toxin (+PTX) for 18 h, and then the Gα_{i1}-YFP fluorescence was measured. *RFU*, relative fluorescence units. *C*, HEK cells were transfected with 5 ng of RGS14-Luc, 250 ng of Gα_{i1}-YFP, and increasing amounts (0, 100, 200, 500, 750, or 1000 ng) of Ric-8A plasmids. Cells were subsequently left alone or pretreated with 100 ng/ml pertussis toxin (+PTX) for 18 h, and then the net BRET between RGS14-Luc and Gα_{i1}-YFP was measured and calculated. *D*, shown is a representative immunoblot of Ric-8A in each sample left alone (*Con*) or treated with PTX (+PTX). Measurements in *B* and *C* were taken from the exact same samples. Data are expressed as the mean of three separate experiments with triplicate determinations.

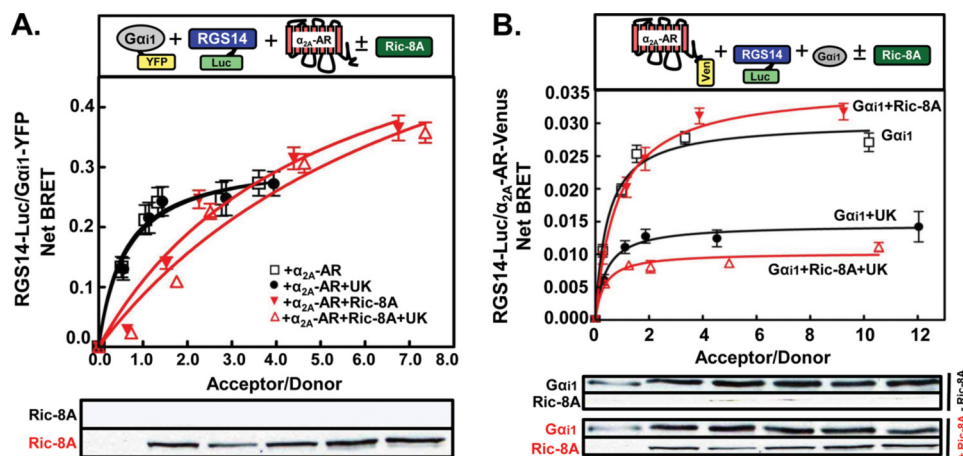


FIGURE 7. Ric-8A induces dissociation of both Gα_{i1} and the α_{2A}-AR from RGS14 after receptor stimulation. *A*, *top panel*, Net BRET signals were generated from the RGS14-Luc/Gα_{i1}-YFP pair in HEK cells transfected with combinations of 5 ng of RGS14-Luc, 500 ng of α_{2A}-AR, 200 ng of Ric-8A, and increasing amounts of Gα_{i1}-YFP (0, 10, 50, 100, 250, and 500 ng) plasmids. Cells were treated with either vehicle or UK14304 (10 μM) for 5 min before BRET signals were measured. *Bottom panel*, shown is a representative immunoblot of Ric-8A expression for all six amounts of Gα_{i1}-YFP plasmid transfected. *Ric-8A* and *Ric-8A* (red) represent lysates from cells without transfected Ric-8A (*top immunoblot*) or cells with transfected Ric-8A (*bottom immunoblot*), respectively. Data are expressed as the mean of three separate experiments with triplicate determinations. *B*, *top panel*, Net BRET signals generated from the RGS14-Luc/α_{2A}-AR-Venus (*Ven*) pair in HEK cells transfected with combinations of 5 ng of RGS14-Luc, 100 ng of Gα_{i1}, 200 ng of Ric-8A, and increasing amounts of α_{2A}-AR-Venus (0, 10, 50, 100, 250, and 500 ng) plasmids. Cells were treated with either vehicle or UK14304 (10 μM) for 5 min before BRET signals were measured. *Bottom panel*, shown is a representative immunoblot of Ric-8A and Gα_{i1} expression for all six amounts of α_{2A}-AR-Venus transfected. Data are expressed as the mean of three separate experiments with triplicate determinations.

effect on the RGS14·α_{2A}-AR complex in the presence of co-expressed Gα_{i1} in the absence of agonist. However, BRET signals between RGS14 and the α_{2A}-AR in the presence of Gα_{i1} and receptor agonist were further reduced by ~25% in the presence of Ric-8A (*red lines*) compared with the absence of Ric-8A (*black lines*) (Fig. 7*B*). These findings suggest that Ric-8A acts to

facilitate dissociation of RGS14 from activated α_{2A}-AR in the presence of Gα_{i1} (see [supplemental Fig. S2C](#)).

DISCUSSION

RGS14 is unusual among RGS protein family members in that it possesses two distinct Gα binding domains; that is, an

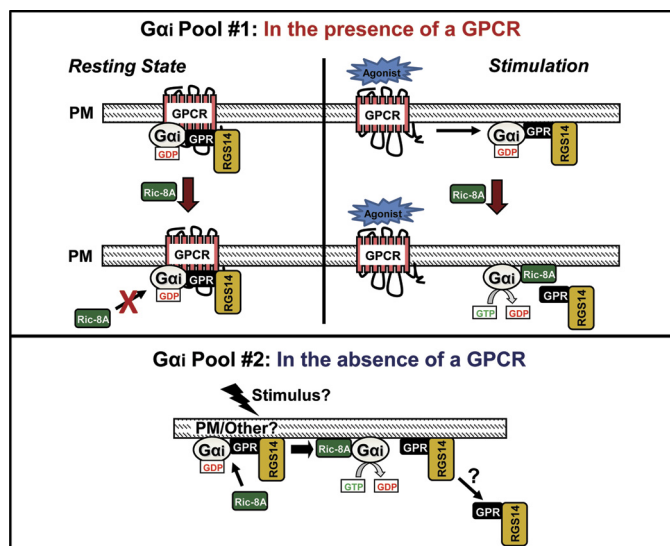


FIGURE 8. Working model depicting Ric-8A regulation of the α_{2A} -AR·Gα_{i1}·RGS14 complex. This visual model includes RGS14, Gα_{i1}, α_{2A} -AR, and Ric-8A localized at or near the plasma membrane (PM). We propose that two pools of Gα_i exist in cells. *Top*, one pool localizes with GPCRs and Gβγ/GPR proteins at the plasma membrane to participate in conventional GPCR-dependent G protein signaling. In the resting state (*left*) of our model, a GPCR·Gα_i·RGS14 complex forms and remains intact. Ric-8A has little effect on this complex in the absence of stimulation. Upon receptor stimulation (*right*), the RGS14·Gα_i complex dissociates from the GPCR, where it can be further acted upon by Ric-8A. *Bottom*, the second Gα_i pool forms complexes with GPR proteins at the plasma membrane in the absence of a GPCR to participate in unconventional GPCR-independent signaling. According to our findings, RGS14 forms a complex with Gα_i through its GPR motif. Ric-8A can recognize this RGS14·Gα_i complex, catalyze GTP exchange on Gα_i, and induce dissociation of the complex.

RGS domain that accelerates GTP hydrolysis on activated Gα_{i/o} subunits (18, 19, 21) and a GPR motif that forms a tight complex with inactive Gα_{i1/3} subunits (17, 19, 25–27). RGS14 also belongs to a second family of signaling proteins, the Group II AGS proteins, which are characterized by the presence of one or more GPR motifs that mediate newly appreciated “unconventional” G protein signaling events (28, 29). Recent studies of AGS3 and AGS4 demonstrate that these GPR domain-containing proteins interact with Gα_i to form complexes with Gα_{i/o}-linked GPCRs in cells (31, 32). Our results with RGS14 support those findings but also highlight some important differences that will be discussed. Overall, our findings indicate the following: 1) RGS14 selectively interacts with Gα_{i1/3} in live cells through its GPR motif, 2) RGS14 forms a Gα_{i/o}-dependent complex with the G_{i/o}-linked α_{2A} -AR in live cells, 3) RGS14 dissociates from the α_{2A} -AR after agonist treatment but remains bound to Gα_{i1}, 4) Ric-8A potentiates agonist-stimulated dissociation of the RGS14· α_{2A} -AR complex, and 5) Ric-8A induces dissociation of Gα_{i1} and α_{2A} -AR from RGS14, having a greater effect in the presence of stimulated α_{2A} -AR. Taken together, these findings suggest that RGS14 integrates both unconventional Ric-8A/G protein signaling and conventional GPCR/G protein signaling. A summary and interpretation of these findings is shown in Fig. 8.

RGS14 Selectively Interacts with Inactive Gα_{i1/3} in Live Cells through Its GPR Motif—Our BRET and confocal imaging indicate that the interaction of RGS14 with inactive Gα_{i1/3} occurs at the plasma membrane of live cells (Fig. 1 and [supple-](#)

[mental Fig S1](#)). Consistent with previous studies (18, 19, 26, 27, 40), the capacity of both Gα_{i1} and Gα_{i3} (but not Gα_{i2}, Gα_o, Gα_s, or Gα_q) to disrupt the BRET between RGS14-Luc and Gα_{i1}-YFP indicates that the observed BRET signal is specific for interactions between RGS14 and Gα_{i1/3} (Fig. 1C).

To clarify which RGS14 domains are involved in the RGS14·Gα_{i1} interaction, we measured the BRET signal between mutant forms of RGS14-Luc and Gα_{i1}-YFP that specifically blocked RGS and/or GPR motif functions (Fig. 2). These studies show that the majority of the observed RGS14·Gα_{i1} interaction is conferred by the GPR motif of RGS14 interacting with Gα_{i1}. The fact that the BRET signal was never completely abolished in the presence of the RGS14 and Gα_{i1} double mutants that ablate Gα binding to both the GPR and RGS domains (Fig. 2, B and C) is consistent with the existence of a third G protein binding site on RGS14, as has been postulated (51).

RGS14 Selectively Interacts with the α_{2A} -AR Receptor in a Gα_{i/o}-dependent Manner—Because RGS14 interacts with Gα_{i/o} family members, we examined whether RGS14 can be regulated by a G_{i/o}-linked GPCR, specifically the α_{2A} -AR. RGS14, Gα_{i1}, and the α_{2A} -AR co-localized at the plasma membrane when all three proteins were expressed together in cells (Fig. 3, *left panel*), consistent with the possibility that a ternary protein complex forms at the plasma membrane. After treatment with the α_{2A} -AR agonist UK14304, RGS14 and Gα_{i1} remained at the plasma membrane, whereas the α_{2A} -AR partially internalized (Fig. 3, *right panel*), suggesting that the ternary complex dissociates. This hypothesis was supported in our BRET experiments. Co-expression of Gα_{i1} resulted in an approximate 3-fold increase in RGS14/ α_{2A} -AR BRET compared with RGS14 and α_{2A} -AR alone (Fig. 4B). The Gα_{i1}-dependent RGS14/ α_{2A} -AR BRET signal was reduced ~50% after receptor activation by agonist, and this agonist effect was blocked by pertussis toxin pretreatment (Fig. 4B, *right panel*). This implies that functional coupling of the α_{2A} -AR to Gα_{i1} disrupts the RGS14· α_{2A} -AR complex. It is possible that the interacting sites between GPCR·Gα_i are different between the inactive and active states, the latter being sensitive to PTX. This is suggested by previous work on the phenomenon of guanine nucleotide-sensitive agonist binding to GPCRs and more recent work demonstrating preformed complexes of GPCRs and G proteins (52, 53).

As expected, RGS14 interaction with the α_{2A} -AR is dependent on the presence of Gα_{i/o} as Gα_q and Gα_s failed to elicit a robust RGS14/ α_{2A} -AR BRET signal. Somewhat unexpectedly, RGS14· α_{2A} -AR association is promoted indiscriminately by the presence of any Gα_{i/o} family member (Gα_{i1}, Gα_{i2}, Gα_{i3}, and Gα_o) (Fig. 4C). This is surprising given that the RGS14· α_{2A} -AR interaction was highly dependent on the GPR motif (Fig. 4D), which only interacts with Gα_{i1} and Gα_{i3} in the absence of receptor. One possible explanation may be that RGS14 recognizes a receptor if the receptor is bound to any Gα_{i/o} protein, reflecting the promiscuity of RGS14 GTPase accelerating protein activity toward activated Gα_{i/o} subunits. In this regard, RGS14 is similar to RGS2. In the absence of receptor, RGS2 acts specifically on Gα_q (54). However, RGS2 is capable of interacting with Gα_i in the presence of a G_{i/o}-linked GPCR (55), albeit with 30-fold lower affinity than for Gα_q (56). We note that

Ric-8A and GPCR Regulation of the RGS14·Gα_{i1} Complex

RGS14 complexes with receptor are dependent on both the G protein and the receptor because the G_s-linked β₂-AR failed to interact with RGS14 in the presence of Gα_{i1} (Fig. 4A).

The GPR motif interaction with Gα_{i1} is important in promoting formation of the RGS14·α_{2A}-AR complex (Fig. 4D). The RGS14/α_{2A}-AR BRET signal was greatly reduced in the presence of RGS14(*GPR-null*) compared with RGS14-WT, indicating that Gα_{i1} has a reduced capacity to bring RGS14 and the α_{2A}-AR in close proximity when it cannot bind the GPR motif. Even when Gα_{i1} could no longer bind either the RGS domain or GPR motif, there was still a slight BRET signal between RGS14(*RGS/GPR-null*) and the α_{2A}-AR. Several possibilities exist to explain these results; 1) there may be another (undefined) Gα_{i1} binding site on RGS14 (51), 2) RGS14 may be bound to Gα_{i1} at a distinct site on the extreme C terminus of Gα_{i1} (17), or 3) an unknown binding partner/scaffold may facilitate an RGS14·α_{2A}-AR interaction.

RGS14 Remains Bound to Gα_{i1} after Dissociating from the α_{2A}-AR—Although RGS14 dissociated from the α_{2A}-AR after agonist treatment in the presence of co-expressed Gα_{i1} (Fig. 4), it remained in complex with Gα_{i1} via the GPR motif (Fig. 5). This finding is unexpected and differs from previous observations that show AGS3 and AGS4 dissociating from Gα_i after receptor activation (Fig. 5A and Refs. 31 and 32)). Our result suggests that RGS14 and Gα_{i1} remain bound after receptor activation. This result is reminiscent of other findings showing that, in contrast to established models of G protein signaling (1), Gβγ may not necessarily always dissociate from Gα. In some cases Gβγ may rearrange relative to Gα-GTP after receptor activation (53), although in others Gβγ does appear to dissociate (Refs. 57–59 and references therein). Irrespective of the mechanism involved, our findings represent a novel mechanism of action for GPCR·Gα·RGS complexes, where the active conformation of the α_{2A}-AR favors release of an RGS14·Gα_{i1} complex that may then be able to function as a signaling complex on its own or with other binding partners (such as potential MAP kinase signaling partners (24)). This complex may be regulated and function independently of the GPCR.

Ric-8A Is a Key Regulator of the GPCR·Gα_{i1}·RGS14 Complex—Although Ric-8A has been shown to influence GPCR signaling (34, 35, 60), little is known mechanistically about if or how Ric-8A may directly interact with and regulate GPCR·G protein complexes. We recently demonstrated that Ric-8A induces dissociation of RGS14 from Gα_{i1} *in vitro* (17). In this study we sought to quantitatively measure the dissociative effects of Ric-8A on RGS14·Gα_i complexes in live cells using BRET (Fig. 6). Pertussis toxin blocked Ric-8A-mediated dissociation of the RGS14·Gα_{i1} complex (Fig. 6, C and D), consistent with recent reports showing that pertussis toxin inhibits Ric-8A GEF activity on Gα_{i1} and that Ric-8A binds to Gα_{i1} at a region overlapping with the pertussis toxin binding site (17, 49). In the absence of pertussis toxin, Ric-8A facilitated RGS14·Gα_{i1} complex dissociation (Fig. 6, C and D). Ric-8A also induced dissociation of the RGS14·Gα_{i1} complex in the presence of the α_{2A}-AR, even in the absence of α_{2A}-AR stimulation (Fig. 7A). This may be explained by Ric-8A effects on Gα_{i1} expression levels. Because Ric-8A overexpression also induced an increase in Gα_{i1} expression (Fig. 6B), it may be that there is an overabun-

dance of Gα_{i1} that is free to bind RGS14. The number of RGS14·Gα_{i1} complexes may, therefore, outnumber the number of α_{2A}-ARs, resulting in free RGS14·Gα_{i1} complexes on which Ric-8A may act in the absence of receptor activation.

Ric-8A did not induce dissociation of the RGS14·α_{2A}-AR complex in the absence of receptor stimulation (Fig. 7B). This is in contrast to its effects on the RGS14·Gα_{i1} complex in the presence of unstimulated receptor. It is possible that Ric-8A facilitates dissociation of RGS14·Gα_{i1} complexes that are not associated with receptors, accounting for the decrease in RGS14/Gα_{i1} BRET seen in the presence of unstimulated receptor (Fig. 7A). In a cellular signaling context, Ric-8A may function similarly to the Arr4 protein in yeast that serves a feed-forward facilitating role in pheromone receptor-G protein signaling mating responses (61). Consistent with this idea is that Ric-8A potentiates taste-receptor signaling by a potential feed-forward mechanism (34).

Taken together, these studies show that RGS14 can associate with a GPCR·Gα_{i/o} complex in a regulated fashion and that Ric-8A is a regulatory partner in this process. Although Ric-8A potentiated dissociation of RGS14·Gα_{i1} complexes from the α_{2A}-AR in both the absence and presence of receptor stimulation, it had no effect on dissociating the RGS14·α_{2A}-AR complex itself in the absence of stimulation. We postulate that two pools of RGS14·Gα_{i1} complexes may exist (Fig. 8). One subset resides at membranes (plasma and others?) in the absence of a GPCR, and the other directly complexes to a cell surface receptor. Ric-8A acts differently on the RGS14·Gα_{i1} complex depending on whether or not the complex is coupled to a GPCR. In the absence of a GPCR (Fig. 8, *bottom*), Ric-8A can recognize and induce dissociation of the RGS14·Gα_{i1} complex. When the RGS14·Gα_{i1} complex is associated with a GPCR (Fig. 8, *top*), Ric-8A may not affect RGS14·Gα_{i1} complexes unless the receptor is activated. In this case Ric-8A induces dissociation of Gα_{i1} from RGS14 and subsequently RGS14 from receptor.

Our findings demonstrate that RGS14 functions in a unique mechanism to integrate both conventional GPCR·G protein signaling and unconventional GPCR-independent G protein signaling. These results highlight newly appreciated roles of GPR proteins at the interface of G protein signaling pathways, making them significant targets in the study of non-canonical G protein regulation and function.

Acknowledgments— We thank Dr. Gregory Tall (University of Rochester School of Medicine and Dentistry) for Ric-8A plasmids and Ric-8A antisera, Dr. Michel Bouvier (University of Montreal) for α_{2A}-AR-Venus and β₂-AR-Venus plasmids, Dr. Stephen Lanier (Medical University of South Carolina) for untagged α_{2A}-AR plasmid, Dr. Thomas Gettys (Pennington Biomedical Research Center, Baton Rouge, LA) for Gα_{i3} and Gα_s antisera, and Dr. Catherine Berlot (Geisenger Institute, Danville, PA) for Gα_s-YFP and Gα_q-YFP plasmids.

REFERENCES

1. Gilman, A. G. (1987) *Annu. Rev. Biochem.* **56**, 615–649
2. Hamm, H. E. (1998) *J. Biol. Chem.* **273**, 669–672
3. De Vries, L., Zheng, B., Fischer, T., Elenko, E., and Farquhar, M. G. (2000) *Annu. Rev. Pharmacol. Toxicol.* **40**, 235–271

4. Hollinger, S., and Hepler, J. R. (2002) *Pharmacol. Rev.* **54**, 527–559
5. Ross, E. M., and Wilkie, T. M. (2000) *Annu. Rev. Biochem.* **69**, 795–827
6. Colombo, K., Grill, S. W., Kimple, R. J., Willard, F. S., Siderovski, D. P., and Gönczy, P. (2003) *Science* **300**, 1957–1961
7. Groves, B., Gong, Q., Xu, Z., Huntsman, C., Nguyen, C., Li, D., and Ma, D. (2007) *Proc. Natl. Acad. Sci. U. S. A.* **104**, 18103–18108
8. Hampoelz, B., and Knoblich, J. A. (2004) *Cell* **119**, 453–456
9. Hess, H. A., Röper, J. C., Grill, S. W., and Koelle, M. R. (2004) *Cell* **119**, 209–218
10. Sans, N., Wang, P. Y., Du, Q., Petralia, R. S., Wang, Y. X., Nakka, S., Blumer, J. B., Macara, I. G., and Wenthold, R. J. (2005) *Nat. Cell Biol.* **7**, 1179–1190
11. Sato, M., Blumer, J. B., Simon, V., and Lanier, S. M. (2006) *Annu. Rev. Pharmacol. Toxicol.* **46**, 151–187
12. Schade, M. A., Reynolds, N. K., Dollins, C. M., and Miller, K. G. (2005) *Genetics* **169**, 631–649
13. Willard, F. S., Kimple, R. J., and Siderovski, D. P. (2004) *Annu. Rev. Biochem.* **73**, 925–951
14. Tall, G. G., Krumins, A. M., and Gilman, A. G. (2003) *J. Biol. Chem.* **278**, 8356–8362
15. Tall, G. G., and Gilman, A. G. (2005) *Proc. Natl. Acad. Sci. U. S. A.* **102**, 16584–16589
16. Thomas, C. J., Tall, G. G., Adhikari, A., and Sprang, S. R. (2008) *J. Biol. Chem.* **283**, 23150–23160
17. Vellano, C. P., Shu, F. J., Ramineni, S., Yates, C. K., Tall, G. G., and Hepler, J. R. (2011) *Biochemistry* **50**, 752–762
18. Cho, H., Kozasa, T., Takekoshi, K., De Gunzburg, J., and Kehrl, J. H. (2000) *Mol. Pharmacol.* **58**, 569–576
19. Hollinger, S., Taylor, J. B., Goldman, E. H., and Hepler, J. R. (2001) *J. Neurochem.* **79**, 941–949
20. Snow, B. E., Antonio, L., Suggs, S., Gutstein, H. B., and Siderovski, D. P. (1997) *Biochem. Biophys. Res. Commun.* **233**, 770–777
21. Traver, S., Bidot, C., Spassky, N., Baltauss, T., De Tand, M. F., Thomas, J. L., Zalc, B., Janoueix-Lerosey, I., and Gunzburg, J. D. (2000) *Biochem. J.* **350**, 19–29
22. Lee, S. E., Simons, S. B., Heldt, S. A., Zhao, M., Schroeder, J. P., Vellano, C. P., Cowan, D. P., Ramineni, S., Yates, C. K., Feng, Y., Smith, Y., Sweatt, J. D., Weinshenker, D., Ressler, K. J., Dudek, S. M., and Hepler, J. R. (2010) *Proc. Natl. Acad. Sci. U. S. A.* **107**, 16994–16998
23. Siderovski, D. P., Diversé-Pierluissi, M., and De Vries, L. (1999) *Trends Biochem. Sci.* **24**, 340–341
24. Shu, F. J., Ramineni, S., and Hepler, J. R. (2010) *Cell. Signal.* **22**, 366–376
25. Kimple, R. J., Kimple, M. E., Betts, L., Sondek, J., and Siderovski, D. P. (2002) *Nature* **416**, 878–881
26. Mittal, V., and Linder, M. E. (2004) *J. Biol. Chem.* **279**, 46772–46778
27. Shu, F. J., Ramineni, S., Amyot, W., and Hepler, J. R. (2007) *Cell. Signal.* **19**, 163–176
28. Blumer, J. B., Oner, S. S., and Lanier, S. M. (2011) *Acta Physiol. (Oxf)*, in press
29. Blumer, J. B., Smrcka, A. V., and Lanier, S. M. (2007) *Pharmacol. Ther.* **113**, 488–506
30. Siderovski, D. P., and Willard, F. S. (2005) *Int. J. Biol. Sci.* **1**, 51–66
31. Oner, S. S., An, N., Vural, A., Breton, B., Bouvier, M., Blumer, J. B., and Lanier, S. M. (2010) *J. Biol. Chem.* **285**, 33949–33958
32. Oner, S. S., Maher, E. M., Breton, B., Bouvier, M., and Blumer, J. B. (2010) *J. Biol. Chem.* **285**, 20588–20594
33. Neitzel, K. L., and Hepler, J. R. (2006) *Semin. Cell Dev. Biol.* **17**, 383–389
34. Fenech, C., Patrikainen, L., Kerr, D. S., Grall, S., Liu, Z., Laugerette, F., Malnic, B., and Montmayeur, J. P. (2009) *Front. Cell. Neurosci.* **3**, 11
35. Nishimura, A., Okamoto, M., Sugawara, Y., Mizuno, N., Yamauchi, J., and Itoh, H. (2006) *Genes Cells* **11**, 487–498
36. Gibson, S. K., and Gilman, A. G. (2006) *Proc. Natl. Acad. Sci. U. S. A.* **103**, 212–217
37. Duzic, E., Coupury, I., Downing, S., and Lanier, S. M. (1992) *J. Biol. Chem.* **267**, 9844–9851
38. Galés, C., Van Durm, J. J., Schaak, S., Pontier, S., Percherancier, Y., Audet, M., Paris, H., and Bouvier, M. (2006) *Nat. Struct. Mol. Biol.* **13**, 778–786
39. Blumer, J. B., Chandler, L. J., and Lanier, S. M. (2002) *J. Biol. Chem.* **277**, 15897–15903
40. Kimple, R. J., De Vries, L., Tronchère, H., Behe, C. I., Morris, R. A., Gist, Farquhar, M., and Siderovski, D. P. (2001) *J. Biol. Chem.* **276**, 29275–29281
41. Hein, P., Rochais, F., Hoffmann, C., Dorsch, S., Nikolaev, V. O., Engelhardt, S., Berlot, C. H., Lohse, M. J., and Bünemann, M. (2006) *J. Biol. Chem.* **281**, 33345–33351
42. Hughes, T. E., Zhang, H., Logothetis, D. E., and Berlot, C. H. (2001) *J. Biol. Chem.* **276**, 4227–4235
43. Hynes, T. R., Mervine, S. M., Yost, E. A., Sabo, J. L., and Berlot, C. H. (2004) *J. Biol. Chem.* **279**, 44101–44112
44. Mercier, J. F., Salahpour, A., Angers, S., Breit, A., and Bouvier, M. (2002) *J. Biol. Chem.* **277**, 44925–44931
45. Khafizov, K. (2009) *J. Mol. Model* **15**, 1491–1499
46. Lan, K. L., Sarvazyan, N. A., Taussig, R., Mackenzie, R. G., DiBello, P. R., Dohlman, H. G., and Neubig, R. R. (1998) *J. Biol. Chem.* **273**, 12794–12797
47. Natchin, M., Gasimov, K. G., and Artemyev, N. O. (2002) *Biochemistry* **41**, 258–265
48. Willard, F. S., Zheng, Z., Guo, J., Digby, G. J., Kimple, A. J., Conley, J. M., Johnston, C. A., Bosch, D., Willard, M. D., Watts, V. J., Lambert, N. A., Ikeda, S. R., Du, Q., and Siderovski, D. P. (2008) *J. Biol. Chem.* **283**, 36698–36710
49. Woodard, G. E., Huang, N. N., Cho, H., Miki, T., Tall, G. G., and Kehrl, J. H. (2010) *Mol. Cell Biol.* **30**, 3519–3530
50. Gabay, M., and Tall, G. G. (2011) *FASEB J.* **25**, 804.805
51. Hepler, J. R., Cladman, W., Ramineni, S., Hollinger, S., and Chidiac, P. (2005) *Biochemistry* **44**, 5495–5502
52. Audet, N., Galés, C., Archer-Lahlou, E., Vallières, M., Schiller, P. W., Bouvier, M., and Pineyro, G. (2008) *J. Biol. Chem.* **283**, 15078–15088
53. Bünemann, M., Frank, M., and Lohse, M. J. (2003) *Proc. Natl. Acad. Sci. U. S. A.* **100**, 16077–16082
54. Heximer, S. P., Watson, N., Linder, M. E., Blumer, K. J., and Hepler, J. R. (1997) *Proc. Natl. Acad. Sci. U. S. A.* **94**, 14389–14393
55. Ingi, T., Krumins, A. M., Chidiac, P., Brothers, G. M., Chung, S., Snow, B. E., Barnes, C. A., Lanahan, A. A., Siderovski, D. P., Ross, E. M., Gilman, A. G., and Worley, P. F. (1998) *J. Neurosci.* **18**, 7178–7188
56. Heximer, S. P., Srinivasa, S. P., Bernstein, L. S., Bernard, J. L., Linder, M. E., Hepler, J. R., and Blumer, K. J. (1999) *J. Biol. Chem.* **274**, 34253–34259
57. Digby, G. J., Lober, R. M., Sethi, P. R., and Lambert, N. A. (2006) *Proc. Natl. Acad. Sci. U. S. A.* **103**, 17789–17794
58. Hollins, B., Kuravi, S., Digby, G. J., and Lambert, N. A. (2009) *Cell. Signal.* **21**, 1015–1021
59. Lambert, N. A. (2008) *Sci. Signal.* **1**, re5
60. Yoshikawa, K., and Touhara, K. (2009) *Chem. Senses* **34**, 15–23
61. Lee, M. J., and Dohlman, H. G. (2008) *Current biology: CB* **18**, 211–215